ACOUSTIC WAVE SCATTERING BY NULL-THICKNESS BODIES WITH COMPLEX GEOMETRY

ANTONIO ROMERO[1], ROCIO VELÁZQUEZ-MATA[1], ANTONIO TADEU[2,3] & PEDRO GALVÍN[1,4]
[1]Escuela Técnica Superior de Ingeniería, Universidad de Sevilla, Spain
[2]Department of Civil Engineering, University of Coimbra, CERIS, Portugal
[3]Itecons, Institute of Research and Technological Development in Construction, Energy, Environment and Sustainability, Portugal
[4]ENGREEN, Laboratory of Engineering for Energy and Environmental Sustainability, Universidad de Sevilla, Spain

ABSTRACT

This paper proposes a general formulation of the BEM based on the Burton–Miller method to study scattering wave propagation by null-thickness bodies with complex geometry. This approach allows the use of arbitrary high-order elements and exact boundary geometry. We use the Bézier–Bernstein form of a polynomial as an approximation basis to represent both geometry and field variables. The solution of the element interpolation problem in the Bézier–Bernstein space defines generalised Lagrange interpolation functions that are used as element shape functions. The proposed procedure consists of a new quadrature rule for the accurate evaluation of integral kernels in the sense of the Cauchy principal and the Hadamard finite part by an exclusively numerical procedure.

Keywords: hypersingular formulation, dual BEM, boundary integral equation, hypersingular kernels, singular kernels.

1 INTRODUCTION

Krishnasamy et al. [1], Liu and Rizzo [2] and Liu [3] developed dual formulations using the Burton–Miller method to study wave scattering from thin shapes. The Burton–Miller method has been widely used to avoid spurious eigenfrequencies in exterior acoustic problems. The method is based on a linear combination of the boundary integral equation (BIE) and the hipersingular boundary integral equation (HBIE) which is typically written as $\text{BIE} + \mu\text{HBIE} = 0$, where μ is the coupling parameter. Although this approach is much simpler and more general than other dual formulations, it has not been widely applied in wave propagation from null-thickness bodies.

2 DUAL BEM FORMULATIONS

This work analyses the wave propagation in a fluid medium in presence of thin rigid bodies with arbitrary shape (Fig. 1) according to the two-dimensional Helmholtz equation:

$$\nabla^2 u(\mathbf{x}) + \kappa^2 u(\mathbf{x}) = 0, \qquad \mathbf{x} \in \Omega, \tag{1}$$

where $u(\mathbf{x})$ is the velocity potential and $\kappa > 0$ denotes the wavenumber. The system is elicited by an incident wavefield caused by a point source defined by $u_0(\mathbf{x}, \mathbf{x}_0) = -\iota H_0^{(1)}(\kappa r_0)/2$, where $H_0^{(1)}$ is the Hankel function of first kind, $r_0 = ||\mathbf{x} - \mathbf{x}_0||$ is the distance to the source point $\mathbf{x}_0$, and the unit imaginary number is denoted by the Greek letter ι to prevent confusion with some subscripts used in the paper.

The problem definition is completed by setting the boundary conditions for on $\Gamma = \partial\Omega$. Dirichlet and Neumann boundary conditions are defined as $u(\mathbf{x}) = \overline{u}(\mathbf{x})$ and $q(\mathbf{x}) = \partial u(\mathbf{x})/\partial \mathbf{n}(\mathbf{x}) = \overline{q}(\mathbf{x})$, respectively, where $\mathbf{n}(\mathbf{x})$ is the outward normal at the boundary. Also, it is possible to adopt the Robin boundary condition to gather the three types of boundary

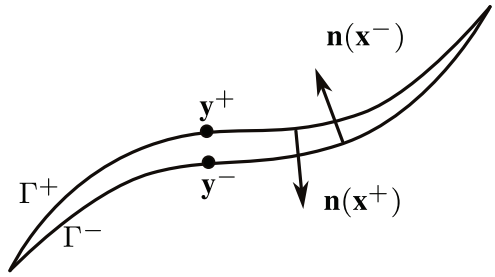

Figure 1: Boundary definition of a thin body.

conditions in one expression:

$$\alpha(\mathbf{x})u(\mathbf{x}) + \beta(\mathbf{x})q(\mathbf{x}) = \gamma(\mathbf{x}), \qquad \mathbf{x} \in \Gamma, \tag{2}$$

where $\alpha(\mathbf{x})$, $\beta(\mathbf{x})$ and $\gamma(\mathbf{x})$ are known parameters [4].

The Green's function $\Psi(\mathbf{x}, \mathbf{y})$ for Helmholtz equation in an unbounded region at receiver position $\mathbf{x}$ due to a source acting at $\mathbf{y}$ is the solution to:

$$\nabla^2\Psi(\mathbf{x}, \mathbf{y}) + \kappa^2\Psi(\mathbf{x}, \mathbf{y}) = -\delta(r) \tag{3}$$

where δ is the Dirac delta function and $r = ||\mathbf{x} - \mathbf{y}||$. The solution to this equation defines the Green's function for an unbounded region in the frequency domain:

$$\Psi(\mathbf{x}, \mathbf{y}) = -\frac{\iota}{4}H_0^{(1)}(\kappa r) \tag{4}$$

It is assumed that κ^2 is not an eigenvalue of $\nabla^2 u(\mathbf{x}) + \kappa^2 u(\mathbf{x}) = 0$ subject to the homogeneous form of the imposed boundary conditions.

2.1 Indeterminacy of the boundary integral equation

This section briefly reviews the degeneracy of the boundary integral equation (BIE) as the thickness of a thin body tends to zero. The BIE for the velocity potential can be written as follows [5]:

$$c(\mathbf{y})u(\mathbf{y}) = u_0(\mathbf{y}) + \int_\Gamma \left(\frac{\partial u(\mathbf{x})}{\partial \mathbf{n}(\mathbf{x})}\Psi(\mathbf{x}, \mathbf{y}) - u(\mathbf{x})\frac{\partial \Psi(\mathbf{x}, \mathbf{y})}{\partial \mathbf{n}(\mathbf{x})} \right) d\Gamma \tag{5}$$

where $\mathbf{y}$ is the collocation point and the integral-free term $c(\mathbf{y})$ depends only on the boundary geometry. The discretised form of eqn (5) when the boundary is discretised into N elements with $\Gamma = \bigcup_{j=1}^{N} \Gamma^j$ is:

$$c(\mathbf{y})u(\mathbf{y}) = u_0(\mathbf{y}) + \sum_{j=1}^{N} \int_{\Gamma^j} \left(\frac{\partial u(\mathbf{x})}{\partial \mathbf{n}(\mathbf{x})}\Psi(\mathbf{x}, \mathbf{y}) - u(\mathbf{x})\frac{\partial \Psi(\mathbf{x}, \mathbf{y})}{\partial \mathbf{n}(\mathbf{x})} \right) d\Gamma \tag{6}$$

Then, the field variables within an element Γ^j are interpolated from the nodal values u^i using element shape functions $\phi^i(\mathbf{x})$ of order p:

$$u(\mathbf{x}) = \sum_{i=0}^{p} \phi^i(\mathbf{x})u^i \tag{7}$$

The element approximation is substituted into eqn (6) to yield the following expression:

$$c(\mathbf{y})u(\mathbf{y}) = u_0(\mathbf{y}) + \sum_{j=1}^{N}\left\{\sum_{i=0}^{p}\left[\left(\int_{\Gamma^j}\phi^i(\mathbf{x})\Psi(\mathbf{x},\mathbf{y})\,d\Gamma\right)q^i - \left(\int_{\Gamma^j}\phi^i(\mathbf{x})\frac{\partial\Psi(\mathbf{x},\mathbf{y})}{\partial\mathbf{n}(\mathbf{x})}\,d\Gamma\right)u^i\right]\right\} \tag{8}$$

which is the classical BEM formulation. This expression for a collocation point $\mathbf{y}^+$ (see Fig. 1) can be further elaborated by separating the element integral according to Γ^+ and Γ^- (a similar equation is obtained for collocation in $\mathbf{y}^-$):

$$\begin{aligned} c(\mathbf{y}^+)u(\mathbf{y}^+) = u_0(\mathbf{y}) &+ \sum_{\Gamma^j\in\Gamma^+}\left\{\sum_{i=0}^{p}\left[\left(\int_{\Gamma^j}\phi^i(\mathbf{x})\Psi(\mathbf{x},\mathbf{y}^+)\,d\Gamma\right)q^i - \left(\int_{\Gamma^j}\phi^i(\mathbf{x})\frac{\partial\Psi(\mathbf{x},\mathbf{y}^+)}{\partial\mathbf{n}(\mathbf{x}^+)}\,d\Gamma\right)u^i\right]\right\} \\ &+ \sum_{\Gamma^j\in\Gamma^-}\left\{\sum_{i=0}^{p}\left[\left(\int_{\Gamma^j}\phi^i(\mathbf{x})\Psi(\mathbf{x},\mathbf{y}^+)\,d\Gamma\right)q^i - \left(\int_{\Gamma^j}\phi^i(\mathbf{x})\frac{\partial\Psi(\mathbf{x},\mathbf{y}^+)}{\partial\mathbf{n}(\mathbf{x}^-)}\,d\Gamma\right)u^i\right]\right\} \end{aligned} \tag{9}$$

Thus, the element nodes are chosen as collocation points to yield a non-symmetric linear system of equations relating the nodal variables. The system of equations is rearranged according to the boundary conditions.

For example, the system of equations for a fixed scatter with null-thickness and sound hard condition, $q(\mathbf{x}) = 0$, $\mathbf{x}\in\Gamma$, can be written as follows:

$$\begin{bmatrix} \frac{1}{2}\mathbf{I}+\mathbf{H}^{++} & -\mathbf{H}^{++} \\ \mathbf{H}^{++} & \frac{1}{2}\mathbf{I}-\mathbf{H}^{++} \end{bmatrix}\begin{Bmatrix}\mathbf{u}^+\\ \mathbf{u}^-\end{Bmatrix} = \begin{Bmatrix}\mathbf{u}_0^+\\ \mathbf{u}_0^-\end{Bmatrix} \tag{10}$$

where, $\mathbf{u}^+$, $\mathbf{u}^-$, $\mathbf{u}_0^+$ and $\mathbf{u}_0^-$ correspond to nodal values of u^i and u_0 at the boundaries Γ^+ and Γ^-. The boundary is assumed to be smooth, i.e. $c(\mathbf{y}^+) = 1/2$. $\mathbf{H}^{++}$ is the influence matrix obtained from the element integration in Γ^+ (second and fourth integrals in eqn (9)) considering that the Green's function satisfies:

$$\frac{\partial\Psi(\mathbf{x},\mathbf{y}^+)}{\partial\mathbf{n}(\mathbf{x}^+)} = -\frac{\partial\Psi(\mathbf{x},\mathbf{y}^+)}{\partial\mathbf{n}(\mathbf{x}^-)} \tag{11}$$

Obviously, the determinant of the coefficient matrix in eqn (10) is equal to zero and the system degenerates.

Similar occurs with the hypersingular boundary integral equation (HBIE). Taking the normal derivative in eqn (9) at the collocation point and assuming a smooth boundary gives:

$$\begin{aligned} \frac{1}{2}\frac{\partial u(\mathbf{y}^+)}{\partial\mathbf{n}(\mathbf{y}^+)} = \frac{\partial u_0(\mathbf{y}^+)}{\partial\mathbf{n}(\mathbf{y}^+)} &+ \sum_{\Gamma^j\in\Gamma^+}\left\{\sum_{i=0}^{p}\left[\left(\int_{\Gamma^j}\phi^i(\mathbf{x})\frac{\partial\Psi(\mathbf{x},\mathbf{y}^+)}{\partial\mathbf{n}(\mathbf{y}^+)}\,d\Gamma\right)q^i - \left(\int_{\Gamma^j}\phi^i(\mathbf{x})\frac{\partial^2\Psi(\mathbf{x},\mathbf{y}^+)}{\partial\mathbf{n}(\mathbf{x}^+)\partial\mathbf{n}(\mathbf{y}^+)}\,d\Gamma\right)u^i\right]\right\} \\ &+ \sum_{\Gamma^j\in\Gamma^-}\left\{\sum_{i=0}^{p}\left[\left(\int_{\Gamma^j}\phi^i(\mathbf{x})\frac{\partial\Psi(\mathbf{x},\mathbf{y}^+)}{\partial\mathbf{n}(\mathbf{y}^+)}\,d\Gamma\right)q^i - \left(\int_{\Gamma^j}\phi^i(\mathbf{x})\frac{\partial^2\Psi(\mathbf{x},\mathbf{y}^+)}{\partial\mathbf{n}(\mathbf{x}^-)\partial\mathbf{n}(\mathbf{y}^+)}\,d\Gamma\right)u^i\right]\right\} \end{aligned} \tag{12}$$

where

$$\frac{\partial^2 \Psi(\mathbf{x}^+, \mathbf{y}^+)}{\partial \mathbf{n}(\mathbf{x}^+) \partial \mathbf{n}(\mathbf{y}^+)} = -\frac{\partial \Psi(\mathbf{x}^-, \mathbf{y}^+)}{\partial \mathbf{n}(\mathbf{x}^-) \partial \mathbf{n}(\mathbf{y}^+)} \tag{13}$$

Then, the system of equation for a fixed scatter with null-thickness and sound hard condition degenerates as in the BIE:

$$\begin{bmatrix} \widetilde{\mathbf{H}}^{++} & -\widetilde{\mathbf{H}}^{++} \\ -\widetilde{\mathbf{H}}^{++} & \widetilde{\mathbf{H}}^{++} \end{bmatrix} \begin{Bmatrix} \mathbf{u}^+ \\ \mathbf{u}^- \end{Bmatrix} = \begin{Bmatrix} \mathbf{q}_0^+ \\ \mathbf{q}_0^- \end{Bmatrix} \tag{14}$$

where $\mathbf{q}_0^+$ and $\mathbf{q}_0^-$ represent the normal derivatives of the point source, $\partial u_0(\mathbf{y}^+)/\partial \mathbf{n}(\mathbf{y}^+)$ and $\partial u_0(\mathbf{y}^-)/\partial \mathbf{n}(\mathbf{y}^-)$, respectively, and the influence matrix $\widetilde{\mathbf{H}}^{++}$ is obtained from element integration.

2.2 Dual formulations

In practice, dual formulations based on the combination of the BIE and HBIE are used to define a well-posed system of equations [1].

The most common procedure is to collocate in a single surface of the scatter (Γ^+ or Γ^-) using both the BIE and the HBIE according to eqns (9) and (12):

$$\begin{aligned} \frac{1}{2}\Sigma u(\mathbf{y}^+) = u_0(\mathbf{y}^+) + \sum_{\Gamma^j \in \Gamma^+} \left\{ \sum_{i=0}^{p} \left[\left(\int_{\Gamma^j} \phi^i(\mathbf{x}) \Psi(\mathbf{x}, \mathbf{y}^+)\, d\Gamma \right) \Sigma q^i \right.\right. \\ \left.\left. - \left(\int_{\Gamma^j} \phi^i(\mathbf{x}) \frac{\partial \Psi(\mathbf{x}, \mathbf{y}^+)}{\partial \mathbf{n}(\mathbf{x}^+)}\, d\Gamma \right) \Delta u^i \right] \right\} \end{aligned} \tag{15}$$

and

$$\begin{aligned} \frac{1}{2}\Delta q(\mathbf{y}^+) = \frac{\partial u_0(\mathbf{y}^+)}{\partial \mathbf{n}(\mathbf{y}^+)} + \sum_{\Gamma^j \in \Gamma^+} \left\{ \sum_{i=0}^{p} \left[\left(\int_{\Gamma^j} \phi^i(\mathbf{x}) \frac{\partial \Psi(\mathbf{x}, \mathbf{y}^+)}{\partial \mathbf{n}(\mathbf{y}^+)}\, d\Gamma \right) \Sigma q^i \right.\right. \\ \left.\left. - \left(\int_{\Gamma^j} \phi^i(\mathbf{x}) \frac{\partial^2 \Psi(\mathbf{x}, \mathbf{y}^+)}{\partial \mathbf{n}(\mathbf{x}^+) \partial \mathbf{n}(\mathbf{y}^+)}\, d\Gamma \right) \Delta u^i \right] \right\} \end{aligned} \tag{16}$$

where $\Sigma u(\mathbf{y}^+) = u(\mathbf{y}^+) + u(\mathbf{y}^-)$ and $\Delta q(\mathbf{y}^+) = q(\mathbf{y}^+) - q(\mathbf{y}^-)$. Similarly, the increment of potential Δu^i and the total flux and Σq^i are defined at the nodal point i. The system of equations for a fixed scatter can be written as:

$$\begin{bmatrix} \frac{1}{2}\mathbf{I} & \mathbf{H}^{++} \\ \mathbf{0} & \widetilde{\mathbf{H}}^{++} \end{bmatrix} \begin{Bmatrix} \Sigma \mathbf{u} \\ \Delta \mathbf{u} \end{Bmatrix} = \begin{Bmatrix} \mathbf{u}_0^+ \\ \mathbf{q}_0^+ \end{Bmatrix} \tag{17}$$

This procedure is commonly referred to as the *dual formulation*. The HBIE equations in (17) can also be used alone if only the increment of the potential $\Delta \mathbf{u}$ needs to be calculated. It should be noted that this approach is only valid for null-thickness scatters and should be further elaborated in presence of thick bodies [6].

Krishnasamy et al. [1], Liu and Rizzo [2] and Liu [3] developed dual formulations using the Burton–Miller method to study wave scattering from thin shapes. The Burton–Miller method has been widely used to avoid spurious eigenfrequencies in exterior acoustic

problems. The method is based on a linear combination of the boundary integral equation (BIE) and the hipersingular boundary integral equation (HBIE) which is typically written as BIE $+ \mu$HBIE $= 0$, where μ is the coupling parameter. Although this approach is much simpler and more general than other dual formulations, it has not been widely applied in wave propagation from null-thickness bodies.

A general formulation of the BEM based on the Burton–Miller method is then proposed to represent acoustic wave propagation problems involving complex thin and thick geometries. The approach presented herein allows the use of arbitrary high-order elements and exact boundary geometry. The proposed method improves the versatility of the BEM as both the BIE and HBIE are evaluated numerically.

2.3 Treatment of singular and hypersingular kernels

The element integrals in eqns (9) and (12) are typically of the form:

$$I = \int_{\Gamma^j} \phi^i(\mathbf{x}) \mathcal{F}(\mathbf{x}, \mathbf{y}) \, d\Gamma(\mathbf{x}) \tag{18}$$

There is an inherent difficulty in boundary element formulations related to the treatment of integral kernels, in particular when the collocation node belongs to the integration element. These integrals are classified as weakly-singular, singular and hypersingular and should be understood in the sense of the Cauchy Principal Value (CPV) or in the Hadamard Finite Part (FP). Combined formulations such as the above become more difficult as all these types of integrals appear, which are typically treated with specific techniques that also depend on the element order. The lack of generality is therefore one of the main drawback on dual formulations.

Kolm and Rokhlin [7] pointed out the need to develop integration schemes that allow evaluation without looking at the integral kernels. The authors presented an algorithm to construct quadrature rules for the simultaneous evaluation of the aforementioned integrals in order to obtain simplified implementations. In this regard, we proposed in a previous work [8] a procedure to design quadrature rules for weakly-singular and singular integrals. Following, the quadrature rules are extended to hypersingular integrals.

The quadrature rules in Velázquez-Mata et al. [8] are derived from the fact that the element shape function $\phi^i(\mathbf{x})$ can be represented in the Bernstein form as [9]:

$$\phi^i(t) = \sum_{k=0}^{n} c_k^i B_k^n(t) \,, \quad i = 0, \ldots, p \tag{19}$$

where c_k^i are control points and $B_k^n(t)$ is the Bernstein polynomial of order n defined over the interval $t \in [0, 1]$:

$$B_k^n(t) = \binom{n}{k} t^k (1-t)^{n-k}, \quad k = 0, \ldots, n \tag{20}$$

Then, the integral kernel in eqn (18) can be rewritten as follows in the natural coordinate ξ:

$$\begin{aligned} I = \int_{-1}^{1} \phi^i(\xi)\mathcal{F}(\xi,\mathbf{y})\frac{d\Gamma}{d\xi}\,d\xi &= \int_{0}^{1} \phi^i(t)\mathcal{F}(t,\mathbf{y})\frac{d\Gamma}{d\xi}\frac{d\xi}{dt}\,dt \\ &= \int_{0}^{1} \left(\sum_{k=0}^{n} c_k^i B_k^n(t)\right)\mathcal{F}(t,\mathbf{y})\frac{d\Gamma}{d\xi}\frac{d\xi}{dt}\,dt \\ &= \sum_{k=0}^{n} c_k^i \left(\int_{0}^{1} B_k^n(t)\mathcal{F}(t,\mathbf{y})\frac{d\Gamma}{d\xi}\frac{d\xi}{dt}\,dt\right) \end{aligned} \tag{21}$$

where, $\mathcal{F}(t,\mathbf{y})$ stands for the type of singularity in the fundamental solution.

This integral can be approximated using a quadrature rule of order M as:

$$\begin{aligned} I &\simeq \sum_{k=0}^{n} c_k^i \left(\sum_{m=0}^{M} B_k^n(t_m)\mathcal{F}(t_m,\mathbf{y})\frac{d\xi}{dt}\frac{d\Gamma(t_m)}{d\xi}w_m\right) \\ &= \sum_{k=0}^{n} c_k^i \left(\sum_{m=0}^{M} \psi_k(t_m,\mathbf{y})\frac{d\Gamma(t_m)}{d\xi}w_m\right) \end{aligned} \tag{22}$$

where t_m and w_m are the integration points and weights, respectively. The quadrature weights are obtained from the solution of a system of equations defined from the above approximation [8]:

$$\sum_{m=0}^{M} \psi_k(t_m,\mathbf{y})w_m = m_k, \qquad k = 0,\ldots,n \tag{23}$$

where m_k are the generalised moment:

$$m_k = \int_{0}^{1} \psi_k(t_m,\mathbf{y})\,dt = \int_{0}^{1} B_k^n(t)\mathcal{F}(t,\mathbf{y})\,dt \tag{24}$$

The generalised moments are the exact solution for the integral kernels in eqn (21) and can be calculated from the Brandaõ approach to the finite part integrals [10], [11].

The hypersingular integral kernels $\mathcal{F}(t,\mathbf{y})$, or its expansion in series, includes terms of the form $1/r^2$, with $r = ||\mathbf{x}-\mathbf{y}||$. The distance r can be expressed in the univariate coordinate as $r = t_0 - 2t + 1$, where t_0 is the coordinate of the collocation point $\mathbf{y}$.

Then, the generalised moment of these terms are obtained according to the following formulas:

$$\begin{aligned} m_k &= \mathrm{FP}\int_{0}^{1} \frac{B_k^n(t)}{(t_0-2t+1)^2}\frac{d\xi}{dt}\,dt \\ &= B_k^n(t_0)\mathrm{FP}\int_{0}^{1} \frac{1}{(t_0-2t+1)^2}\frac{d\xi}{dt}\,dt - \frac{dB_k^n(t_0)}{dt}\frac{dt}{d\xi}\mathrm{CPV}\int_{0}^{1} \frac{1}{t_0-2t+1}\frac{d\xi}{dt}\,dt \\ &+ \int_{0}^{1} \frac{B_k^n(t) - B_k^n(t_0) + \dfrac{dB_k^n(t_0)}{dt}\dfrac{dt}{d\xi}(t_0-2t+1)}{t_0-2t+1}\frac{d\xi}{dt}\,dt \end{aligned} \tag{25}$$

where

$$\mathrm{FP}\int_0^1 \frac{1}{(t_0-2t+1)^2}\frac{d\xi}{dt}\,dt = \begin{cases} 2/(t_0^2-1) & |t_0|\neq 1 \\ -1/2 & t_0=\pm 1 \end{cases} \tag{26}$$

$$\mathrm{CPV}\int_0^1 \frac{1}{t_0-2t+1}\frac{d\xi}{dt}\,dt = \begin{cases} \log\left|\dfrac{t_0+1}{1-t_0}\right| & |t_0|\neq 1 \\ \pm\log(2) & t_0=\pm 1 \end{cases} \tag{27}$$

Eqn (23) defines a system of $n+1$ equations for each type of function to be integrated. The extension of the quadrature rule proposed in this work is capable of integrating kernels with constant, $\log(r)$, $1/r$, and $1/r^2$ terms when the collocation point belongs to the integration element, which are found in the fundamental solution or in their series expansions. Therefore, eqn (23) defines a system of $4(n+1)$ equations with $M+1$ unknown weights w_m. The solution is obtained in the least-squares sense when overdetermined and in the minimum norm least-squares sense when undetermined. The solution of the generalised moment for weakly singular and singular integrals can be found in Velázquez-Mata et al. [8].

2.4 Dealing with complex boundary geometry

The BEM formulation in the Bézier–Bernstein space [4], [9] is used in this work to handle exact geometries defined as Bézier curves, that are widely used in computer aid design (CAD). The element geometry is then represented as $\Gamma^j(\mathbf{x}) = \mathbf{r}_n^j(t)$, where the Bézier curves is defined as follows:

$$\mathbf{r}_n^j(t) = \sum_{k=0}^{n} \mathbf{b}_k^j B_k^n(t) \tag{28}$$

with $\mathbf{b}_k^j$ the control points used to approximate the geometry and n the curve degree. Then, the element integral (eqn (18)) is rewritten in the univariate basis as [9]:

$$I = \int_{\Gamma^j} \phi^i(\xi)\mathcal{F}(\xi,\mathbf{y})\,d\Gamma = \int_0^1 \phi^i(\xi)\mathcal{F}(\xi,\mathbf{y})\left|\frac{d\mathbf{r}_n^j(t)}{dt}\right| dt \tag{29}$$

An efficient curve computation of $\mathbf{r}_n^j(t)$ is achieved using the polar form (or blossom) [12], which defines a multi-affine transformation satisfying:

$$\mathbf{b}_k^j = \mathbf{R}^j(\underbrace{0,\ldots,0}_{n-k},\underbrace{1,\ldots,1}_{k}) \tag{30}$$

where $\mathbf{R}^j(t_1,\ldots,t_n)$ is computed as:

$$\mathbf{R}^j(t_1,\ldots,t_n) = \sum_{\substack{I\cap K=\emptyset \\ I\cup K=\{1,2,\ldots,n\}}} \prod_{i\in I}(1-t_i)\prod_{k\in K} t_k \mathbf{b}^j_{|K|} \tag{31}$$

Thus, the Bézier in the polar form is defined as follows:

$$\mathbf{r}_n^j(t) = \sum_{k=0}^{n} \mathbf{R}^j(\underbrace{0,\ldots,0}_{n-k},\underbrace{1,\ldots,1}_{k})B_k^n(t) = \mathbf{R}^j(t,\ldots,t) \tag{32}$$

and its first derivative becomes:

$$\frac{d\mathbf{r}_n^j(t)}{dt} = \frac{d}{dt}\mathbf{R}^j(t,\ldots,t) = n\big(\mathbf{R}^j(\underbrace{t,\ldots,t}_{n-1},1) - \mathbf{R}^j(0,\underbrace{t,\ldots,t}_{n-1})\big) \tag{33}$$

Boundary elements are defined by subdividing Bézier curves according to a h-refinement strategy. The element geometry is evaluated and subdivided using the polar form of Bernstein polynomials without CAD interaction, providing great flexibility in mesh refinement. The field variables are approximated independently of the geometry representation, and therefore p-refinement only affects the field approximation.

2.5 System of equations

The system of equations is obtained from the discretised boundary integral equation according to the element approximation. Neumann and Robin boundary conditions are defined in scattering problems to define sound hard and impedance conditions from eqn (2):

$$\frac{\partial u(\mathbf{x})}{\partial \mathbf{n}(\mathbf{x})} = \frac{\gamma(\mathbf{x}) - \alpha(\mathbf{x})u(\mathbf{x})}{\beta(\mathbf{x})} \tag{34}$$

The boundary conditions can be implicitly defined in the integral kernels, rather than by prescribing nodal values as is done in standard formulations [4]. The main advantage of this procedure is that the right-hand side of the system of equations is integrated taking the exact distribution of loads into account. Then, eqn (6) becomes:

$$\begin{aligned}\frac{1}{2}u(\mathbf{y}) + \sum_{j=1}^{N}\left[\int_{\Gamma^j}\left(\frac{\alpha(\mathbf{x})}{\beta(\mathbf{x})}\Psi(\mathbf{x},\mathbf{y}) + \frac{\partial\Psi(\mathbf{x},\mathbf{y})}{\partial\mathbf{n}(\mathbf{x})}\right)u(\mathbf{x})\,d\Gamma\right] \\ = \sum_{j=1}^{N}\left[\int_{\Gamma^j}\frac{\gamma(\mathbf{x})}{\beta(\mathbf{x})}\Psi(\mathbf{x},\mathbf{y})\,d\Gamma\right] + u_0(\mathbf{y})\end{aligned} \tag{35}$$

Once the element approximation (eqn (7)) is introduced in (35), a system of equations $\mathbf{Hu} = \mathbf{b}$ is obtained which allows the solution of the unknown nodal values $\mathbf{u}$. Similarly, a system of equation is $\widetilde{\mathbf{H}}\mathbf{u} = \widetilde{\mathbf{b}}$ is derived from the HBIE (eqn (12)):

$$\begin{aligned}-\frac{\alpha(\mathbf{y})}{2\beta(\mathbf{y})}u(\mathbf{y}) + \sum_{j=1}^{N}\left[\int_{\Gamma^j}\left(\frac{\alpha(\mathbf{x})}{\beta(\mathbf{x})}\frac{\partial\Psi(\mathbf{x},\mathbf{y})}{\partial\mathbf{n}(\mathbf{y})} + \frac{\partial^2\Psi(\mathbf{x},\mathbf{y})}{\partial\mathbf{n}(\mathbf{x})\partial\mathbf{n}(\mathbf{y})}\right)u(\mathbf{x})\,d\Gamma\right] \\ = -\frac{\gamma(\mathbf{y})}{2\beta(\mathbf{y})} + \sum_{j=1}^{N}\left[\int_{\Gamma^j}\frac{\gamma(\mathbf{x})}{\beta(\mathbf{x})}\frac{\partial\Psi(\mathbf{x},\mathbf{y})}{\partial\mathbf{n}(\mathbf{y})}\,d\Gamma\right] + \frac{\partial u_0(\mathbf{y})}{\partial\mathbf{n}(\mathbf{y})}\end{aligned} \tag{36}$$

Finally, the system of equation given by the Burton–Miller method using a linear combination of eqns (35) and (36) is $(\mathbf{H} + \mu\widetilde{\mathbf{H}})\mathbf{u} = \mathbf{b} + \mu\widetilde{\mathbf{b}}$, where μ is the coupling parameter.

The proposed method is valid for both thick and thin geometries. The boundary is represented by overlapping curves with outward normals in the limit case of zero thickness. The procedure for obtaining the system of equations and the solution is the same regardless of the boundary geometry. Therefore, the proposed BEM formulation is simplest and most general approach for dealing with arbitrary geometries.

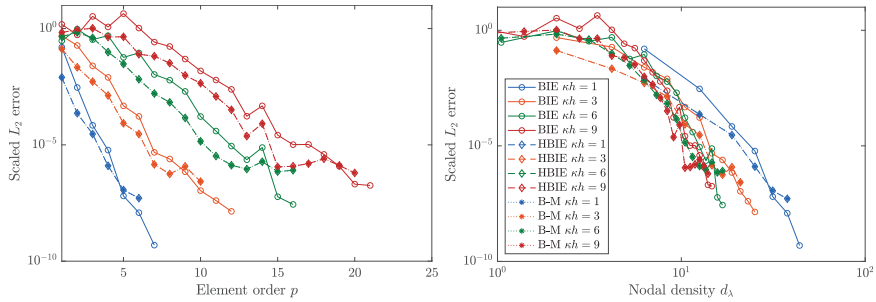

(a) (b)

Figure 2: Convergence analysis for hp-refinement plotted versus (a) element order p; and (b) nodal density per wavelength d_λ.

3 CHOOSING THE COUPLING PARAMETER

Many authors have discussed the choice of the coupling parameter μ as referred to by Marburg in [13]. The parameter $\mu = \pm\iota/\kappa$ is assumed to provide the system with the lowest condition number. Marburg [13] discussed that the correct sign of the coupling parameter depends on the harmonic time dependence and on the Green's function. Liu [3] suggests that using $\mu = \pm\iota h$ improves the contribution from both formulations, as the element length h should decrease with increasing wavenumber. The author concludes that this choice improves the system conditioning and the stability of the results.

However, the choice of the coupling parameter for thin bodies has not been investigated as much in the past. The main contributions can be found in the early work of Rizzo and co-workers. Krishnasamy et al. [1] set $\mu = 1$ to study acoustic wave propagation through a thin penny-shaped scatterer with radius $a = 1$ and thickness up to $h = 10^{-7}$. Later, Liu and Rizzo [2] analysed shear waves in a penny-shaped open crack of different thicknesses and found that the choice of coupling parameter was not so restrictive. Values between $\mu = -1$ and $\mu = +1$ gave well-posed systems with low condition numbers.

This section study the optimum choice of the coupling parameter for thick and thin bodies.

3.1 Optimal choice of the coupling parameter for thick bodies

First, we considered a benchmark problem concerning the scattering of waves from a fixed cylindrical cavity at the origin with radius $r = 1\,\text{m}$ elicited by a source point in $\mathbf{y} = (0, 1)$. The circular geometry was approximated by a C^2 quartic Bézier curve [9]. The analytical solution to this problem can be found in Tadeu and Godinho [14].

Fig. 2 shows the L_2 scaled error ϵ_2 for $\kappa = 40\,\text{rad/m}$ and different $hp-$strategies. A convergence analysis was carried out for several element sizes h with successive $p-$enrichment. The element discretisation was set to $\kappa h = \{1,\ 3,\ 6,\ 9\}$, resulting in six, two, one and one-and-a-half elements per wavelength according to the node density:

$$d_\lambda = \frac{2\pi p}{\kappa h} \tag{37}$$

The boundary elements were then discretised to perform a $h-$ refinement and the element order was increased until convergence was reached. The coupling parameter was $\mu = -\iota h$ to account for the element length in the mesh refinements.

The lowest error was $\mathcal{O}(10^{-10})$ for the BIE formulation and $\mathcal{O}(10^{-8})$ for the HBIE and the Burton–Miller formulations. The accuracy of the Burton–Miller formulation was the same as that of the HBIE. Furthermore, the convergence was faster for the finer discretisation than for the coarser discretisation. The numerical results converged to the analytical solution when the node density per wavelength was higher than $d_\lambda = 3$ in the coarser meshes and $d_\lambda = 12$ for the finest discretisation. Furthermore, the solution error for a fixed node density was lower for a coarse mesh than for a fine mesh, as can be seen in Fig. 2(b). Therefore, a coarse mesh with an adequate node density gave better results than a fine mesh with the same density, or equivalently, the use of high order elements in coarse meshes (p-refinement) gave better results than low order elements in a fine discretisation (h-refinement) for a fixed node density.

We have found in several tests that the accuracy of the Burton–Miller method depends strongly on the choice of the coupling parameter. Although the most common choices such as $\mu = -\iota h$ or $\mu = \iota/\kappa$ give good results, there are other options that provide more accurate results. This issue requires further research to properly identify the optimal coupling parameter that minimises the solution error. The optimum choice of the coupling parameter was found as the optimal solution to this problem using a genetic algorithm. The polar form of the coupling parameter $\mu = \rho\angle\theta = \rho(\cos(\theta) + \iota\sin(\theta))$ was adopted for this analysis. The lower and upper limits of the optimisation variables were $\rho \in [0, 100]$ and $\theta \in [0, 2\pi]$. The initial population was 50, the crossover fraction was 0.8, and the elite children were 3 in each generation.

Fig. 3(a) compares the error for a wavenumber varying in the interval $\kappa \in [1,\ 80]$ rad/m obtained with the Burton–Miller method using the coupling parameters $\mu = -\iota/h$, $\mu = -\iota\kappa$ and the optimum choice $\mu = \rho\angle\theta$. The boundary discretisation was given by $\kappa h = 9$ with a node density $d_\lambda = 10$, which corresponds to one-and-a-half elements per wavelength of order $p = 15$. The error was $\mathcal{O}(10^{-6})$ for the common choices $\mu = -\iota/h$ and $\mu = -\iota\kappa$ of the coupling parameter. However, the error was $\mathcal{O}(10^{-10})$ for the optimal choice. Fig. 3(b) shows the radius and angle of the optimal coupling parameter. This fact requires further investigation.

Finally, Fig. 4 shows the scattered wavefield by degenerated ellipse with the minor axis tending to zero. The radial distribution of the incident wave field in the absence of the scatterer was lost under the effect of boundary wave reflections. A shadowed region was found downstream the scatterers in all cases where the potential amplitude was significantly lower.

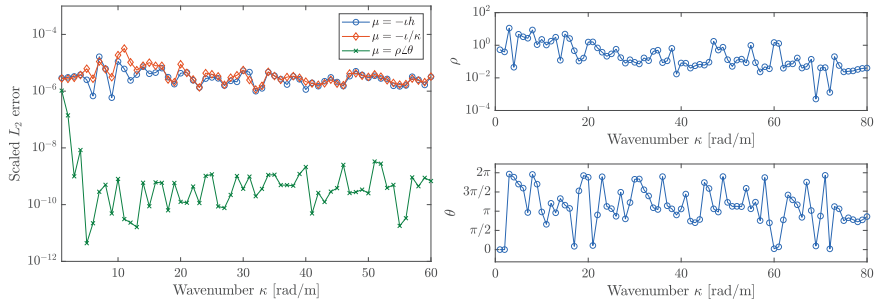

(a) (b)

Figure 3: (a) Scaled L_2 error for different choices of the coupling parameter; and (b) Optimal coupling parameter $\mu = \rho\angle\theta$.

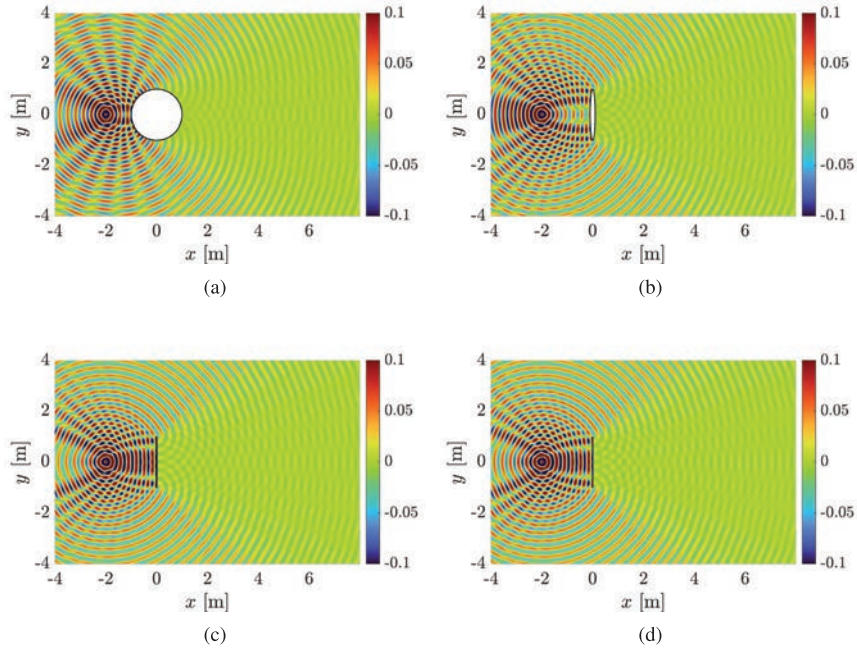

Figure 4: Real part of potential field distribution for ellipse geometries given by: (a) $R_x = 1.00\,\text{m}$; (b) $R_x = 0.10\,\text{m}$; (c) $R_x = 0.01\,\text{m}$; and (d) $R_x = 0.00\,\text{m}$.

4 CONCLUSIONS

This paper analysed the application of the Burton–Miller method to study wave scattering by thick or thin bodies with complex geometry. The proposed method is based on the Bézier–Bernstien formulation of the BEM. The approach allows the use of arbitrary high-order element and exact boundary geometry. The singular and hypersingular kernels are numerically evaluated without the need for a regularisation process. This approach is much simpler and more general than other dual formulations and improves the versatility of the BEM as both the BIE and HBIE are evaluated numerically. The procedure for obtaining the system of equations and the solution is the same regardless of the boundary geometry. Therefore, the proposed BEM formulation is the simplest and most general approach for dealing with arbitrary geometries.

ACKNOWLEDGEMENTS

The authors would like to acknowledge the financial support provided by the Spanish Ministry of Science and Innovation under the research project PID2022-138674OB-C21, PROYEXCEL_00659 funded by Regional Ministry of Economic Transformation, Industry, Knowledge and Universities of Andalusia, and the Andalusian Scientific Computing Centre (CICA).

REFERENCES

[1] Krishnasamy, G., Rizzo, F.J. & Liu, Y., Boundary integral equations for thin bodies. *International Journal for Numerical Methods in Engineering*, **37**(1), pp. 107–121, 1994.

[2] Liu, Y. & Rizzo, F., Scattering of elastic waves from thin shapes in three dimensions using the composite boundary integral equation formulation. *Journal of the Acoustical Society of America*, **102**(2 pt 1), pp. 926–932, 1997.
[3] Liu, Y., On the BEM for acoustic wave problems. *Engineering Analysis with Boundary Elements*, **107**, pp. 53–62, 2019.
[4] Romero, A., Galvín, P. & Tadeu, A., An accurate treatment of non-homogeneous boundary conditions for development of the BEM. *Engineering Analysis with Boundary Elements*, **116**, pp. 93–101, 2020.
[5] Wu, T., *Boundary Element Acoustics Fundamentals and Computer Codes. Advances in Boundary Elements*, WIT Press: Southampton and Boston, 2000.
[6] Toledo, R., Aznárez, J., Greiner, D. & Maeso, O., Shape design optimization of road acoustic barriers featuring top-edge devices by using genetic algorithms and boundary elements. *Engineering Analysis with Boundary Elements*, **63**, pp. 49–60, 2016.
[7] Kolm, P. & Rokhlin, V., Numerical quadratures for singular and hypersingular integrals. *Computers and Mathematics with Applications*, **41**(3), pp. 327–352, 2001.
[8] Velázquez-Mata, R., Romero, A., Domínguez, J., Tadeu, A. & Galvín, P., A novel high-performance quadrature rule for BEM formulations. *Engineering Analysis with Boundary Elements*, **140**, pp. 607–617, 2022.
[9] Romero, A., Galvín, P., Cámara-Molina, J. & Tadeu, A., On the formulation of a BEM in the Bézier–Bernstein space for the solution of Helmholtz equation. *Applied Mathematical Modelling*, **74**, pp. 301–319, 2019.
[10] Brandao, M.P., Improper integrals in theoretical aerodynamics: The problem revisited. *AIAA Journal*, **25**(9), pp. 1258–1260, 1987.
[11] Carley, M., Numerical quadratures for singular and hypersingular integrals in boundary element methods. *SIAM Journal on Scientific Computing*, **29**(3), pp. 1207–1216, 2007.
[12] Ramshaw, L., *Blossoming: A Connect-the-Dots Approach to Splines*. Digital Equipment Corporation SRC Report No. 19, 1987.
[13] Marburg, S., The Burton and Miller method: Unlocking another mystery of its coupling parameter. *Journal of Computational Acoustics*, **24**(1), 2016.
[14] Tadeu, A. & Godinho, L., Three-dimensional wave scattering by a fixed cylindrical inclusion submerged in a fluid medium. *Engineering Analysis with Boundary Elements*, **23**(9), pp. 745–755, 1999.
[15] Hur, S. & Kim, T.W., The best G1 cubic and G2 quartic Bézier approximations of circular arcs. *Journal of Computational and Applied Mathematics*, **236**(6), pp. 1183–1192, 2011.